Pharm Res (2014) 31:2326–2334
DOI 10.1007/s11095-014-1329-z

RESEARCH PAPER

In Vitro Efficacy of Polysaccharide-Based Nanoparticles Containing Disease-Modifying Antirheumatic Drugs

Nan Zhang • Patricia R. Wardwell • Rebecca A. Bader

Received: 17 June 2013 / Accepted: 8 February 2014 / Published online: 5 March 2014

ABSTRACT

Purpose To evaluate the therapeutic efficacy of dexamethasone (DM) and methotrexate (MTX) entrapped within polysialic acid (PSA)-trimethyl chitosan (TMC) nanoparticles using an *in vitro* model of rheumatoid arthritis (RA).

Methods The loading capacity of the PSA-TMC nanoparticles was determined. An RA *in vitro* model was developed by stimulating a synovial cell line with a proinflammatory mediator. Multiplex immunoassay was used to determine changes in the secretion of interleukin-6 (IL-6), interleukin-8 (IL-8), and granulocyte-macrophage colony-stimulating factor (GM-CSF) by the *in vitro* model following administration of the DM- and MTX-loaded nanoparticles.

Results The loading capacity of the PSA-TMC nanoparticles was approximately 0.1 mg of drug/mg of nanoparticle. When applied to our *in vitro* model of RA, there were no significant differences in the concentrations of IL-6 and IL-8 when comparing the free drugs and drug-loaded nanoparticles, administered at concentration of 0.1 mg/ml and 1.0 mg/ml, respectively.

Conclusions The present study verified that MTX and DM are able to retain bioactivity when loaded into PSA-TMC nanoparticles. Although *in vitro* efficacy was not increased, the *in vivo* efficacy will likely be enhanced by the site-specific targeting conferred by nanoparticle entrapment.

KEY WORDS chitosan · drug delivery · nanoparticles · polysialic acid · rheumatoid arthritis

Electronic supplementary material The online version of this article (doi:10.1007/s11095-014-1329-z) contains supplementary material, which is available to authorized users.

N. Zhang • P. R. Wardwell • R. A. Bader (✉)
Syracuse Biomaterials Institute
Department of Biomedical and Chemical Engineering
Syracuse University, 318 Bowne Hall
Syracuse, New York 13244, USA
e-mail: babader@syr.edu

ABBREVIATIONS

DM	Dexamethasone
DMARD	Disease-Modifying Antirheumatic Drug
GM-CSF	Granulocyte-Macrophage Colony-Stimulating Factor
IL-1β	Interleukin-1β
IL-6	Interleukin-6
IL-8	Interleukin-8
MTX	Methotrexate
PSA	Polysialic Acid
RA	Rheumatoid Arthritis
TMC	Trimethyl chitosan
TPP	Tripolyphosphate

INTRODUCTION

Conventional therapeutics for rheumatoid arthritis (RA) are plagued by severe, potentially life threatening consequences as a result of non-specific organ toxicity (1,2). For example, methotrexate (MTX), the current gold standard in RA treatment, has been in use as an oncology drug since 1950 and as a disease-modifying antirheumatic drug (DMARD) since 1970. Although the mechanism of action in RA remains largely unclear, MTX is speculated to either reduce proliferation of infiltrating inflammatory cells or suppress the release of pro-inflammatory mediators (3). The drug is recognized to be hepatotoxic and patients undergoing treatment receive periodic liver function tests and liver biopsies. Despite the latter precautions, cirrhosis and fibrosis are known side effects, and fatalities have been reported (4,5). Furthermore, the bioavailability, as well as the peak serum concentration, of orally administered MTX varies considerably between patients. The large variability in pharmacokinetic parameters likely contributes to the observed toxicity (1,2). Likewise, dexamethasone (DM), a widely used glucocorticosteroid, is associated with severe side effects, including insulin resistance and

osteoporosis (6). Given the high incidence of adverse side effects, in conjunction with the variability in drug effectiveness, a number of investigators have sought to identify a carrier system that favors DMARD delivery to the inflamed joint tissue, minimizes concurrent organ toxicity, and improves the pharmacokinetic properties.

In designing an appropriate drug delivery system for RA, a lack of immunogenicity and non-cytotoxicity are requisite material properties. Polysaccharides are a logical, versatile choice for the formation of biodegradable, non-immunogenic nanoparticles. Due to variations in chemical composition, polysaccharides exhibit overall neutral, negative, or positive charge states. In addition, the macromolecular chains possess a number of functionalities, particularly amines, hydroxyl groups, and carboxylic acids that are easily amenable to modification (7). Although a number of polysaccharides have been explored, chitosan is the most used polysaccharide in the realm of targeted drug delivery (8). Often, the cationic free or quaternized primary amines of the polymer are used for ionic crosslinking through a polyanion crosslinker, such as tripolyphosphate (TPP) (9–12). Chitosan can also be electrostatically associated with negatively charged natural polymers, such as hyaluronic acid, alginate, heparin, peptides, and nucleic acids (7).

As previously reported, our laboratory has developed nanoparticles *via* complexation of N-trimethyl chitosan (TMC) with a unique polysaccharide, polysialic acid (PSA), in the presence of TPP. By incorporating PSA, nanoparticles were obtained with a smaller size relative to previously developed chitosan and TMC nanoparticulate systems (13). Based upon the pioneering work of Gregoriadis *et al.* in the development of PSA-therapeutic conjugates (14–18), PSA functions to prevent undesirable uptake by the reticuloendothelial system, thereby extending circulatory stability and facilitating site-specific delivery of associated therapeutics by passive accumulation in areas of leaky vasculature, such as tissue affected by RA (19–21). Despite demonstrated success, colloidal carrier systems offer an advantage over previously designed PSA conjugates in that the bioactivity of the entrapped therapeutic can be more readily retained.

This study aims to verify that two DMARDs, MTX and DM, remain therapeutically effective when entrapped within the previously developed PSA-TMC nanoparticles (13). MTX- and DM-loaded nanoparticles were administered to an *in vitro* model of RA generated from interleukin-1β (IL-1β) activated SW-982 synovial cells. Following treatment of the *in vitro* model for 24 h, the concentrations of the following pro-inflammatory proteins within the supernatant were evaluated using multiplex immunoassay on the Luminex® Platform: interleukin-6 (IL-6), interleukin-8 (IL-8), and granulocyte-macrophage colony-stimulating factor (GM-CSF). The three proteins chosen are representative of the pro-inflammatory cytokines, chemokines, and growth factors that are upregulated in those that suffer from RA (22,23).

MATERIALS AND METHODS

Materials

Polysialic acid (PSA) was purchased from Nacalai USA, Inc. (San Diego, CA, USA). Sodium hydroxide (extra pure, pellets), sodium tripolyphosphate (pure, TPP), acetonitrile (HPLC grade), and chitosan (Mw 100 Da−300 kDa) were obtained from Acros Organics (New Jersey, USA). Sodium iodide (puriss), methyl iodide (reagent plus), 1-methyl-2-pyrrolidinone (anhydrous), ethanol (re- agent alcohol), ammonium acetate, deuterium oxide, and acetic acid (ACS reagent grade) were procured from Sigma (St. Louis, MO, USA). Hydrochloric acid (ACS plus grade) was acquired from Fisher Scientific (Hanover Park, IL, USA). MTX and DM were purchased from Enzo Life Science (Farmingdale, NY, USA). All chemical reagents were used without further purification.

Cell Culture

The SW-982 human synovial sarcoma cell line was acquired from ATCC (Manassas, VA). Dulbecco's Modified of Eagle's Medium (DMEM) supplemented with 4.5 g/L glucose, L-glutamine & sodium pyruvate was procured from Mediatech, Inc. (Manassas, VA). Fetal bovine serum (FBS) and penicillin-streptomycin were purchased from Lonza, Inc. (Allendale, NJ). Alexa Fluor® 488 was obtained from Life Technologies (Grand Island, NY).

Preparation and Characterization of DMARD-Loaded PSA-TMC Nanoparticles

Drug-loaded PSA-TMC nanoparticles were prepared from PSA and TMC (55% degree of substitution) following a previously published protocol (13). Briefly, 6.4 mg of TMC were dissolved in 3 ml of 0.3% acetic acid in a glass vial. In a separate glass vial, 3.2 mg of PSA, 1 mg of TPP, and 2.4 mg of MTX or DM were mixed well in 2 ml of DI water. The PSA solution was sonicated for 10 min and then added drop-wise to the TMC solution with stirring. Stirring was continued for 30 min to ensure nanoparticle formation. For DM, non-encapsulated drug was removed by centrifuging at 1,000 rpm for 5 min prior to nanoparticle isolation. The DM pellet was retained to assess the loading properties of the nanoparticles, while the collected supernatant was subsequently used to obtain DM-loaded nanoparticles. MTX has higher aqueous solubility and could, therefore, not be removed *via* centrifugation, as previously reported (13). Centrifugation for 15 min at 3,000 rpm yielded MTX- or DM-

loaded nanoparticles as a white pellet. Similar to the procedure previously described for MTX (13), an Ultrafast Liquid Chromatography System (UFLC, Shimadzu Scientific Instruments, Japan) equipped with an SPD-20AV UV detector, an SIL- 20A autosampler, a DGU-20A3 degasser, and a Shimpack XR-ODS/C8/Phenyl column was used to quantify the amount of DM that was not encapsulated and acquired upon centrifugation at 1,000 rpm. The mobile phase was a 70:30 mixture (v/v) of water:acetonitrile, and the detection wavelength was set to 238 nm. A calibration curve were constructed by using PeakFit 4.2 software to determine the area under the peak of at least five known concentrations of free drug in the mobile phase ranging from 0.39 mg/L to 100 mg/L. Loading efficiency (LE) and loading capacity (LC) were determined with the following equations:

$$\mathrm{LE} = \frac{m_{DM,added} - m_{DM,unencapsulated}}{m_{DM,added}} \times 100 \quad (1)$$

$$\mathrm{LC} = \frac{m_{DM,added} - m_{DM,unencapsulated}}{m_{Nanoparticles}} \quad (2)$$

where $m_{DM,added}$ is the mass of DM added to the PSA solution, $m_{DM,unencapsulated}$ is the mass of DM that has not been encapsulated into the nanoparticles, and $m_{Nanoparticles}$ is the mass of the nanoparticles used for DM loading.

The sizes and zeta potentials of DMARD-loaded PSA-TMC nanoparticles were measured *via* a Malvern Zetasizer NanoZS90 (Malvern Instruments Ltd., Malvern, UK). The size distribution of nanoparticles was reported as the polydispersity index (PDI). Nanoparticles were suspended in DI water at a concentration of 2 mg/ml and transferred into disposable microcuvettes and disposable capillary cells (Malvern Instruments Ltd., Malvern, UK) for size and zeta potential measurements, respectively. For dynamic light scattering, the temperature was set to 25°C and scattered light was detected at 173°. All measurements were performed in triplicate.

The release profile of DM from the PSA-TMC nanoparticles was determined in a manner identical to that previously reported for MTX (13). In brief, isolated nanoparticles were resuspended in 5 ml of DI water, and the resultant solution was transferred to dialysis tubes with a large MWCO of 12,000–14,000 (Spectrum Laboratories, Rancho Dominguez, CA, USA). The dialysis tube was placed in 45 ml of DI water at 37°C without shaking. At select time intervals from 10 min to 48 h, 1 ml of external medium was withdrawn and replaced with fresh medium. The amount of DM released at each time interval was established *via* UFLC using the conditions described above.

In Vitro Cytotoxicity of Nanoparticles

WST-8 assay (Cayman Chemical Company, Ann Arbor, MI) was conducted on the SW-982 cell line, following the manufacturer's instructions, to assess the cytotoxicity of the drug-loaded nanoparticles. Cells were seeded into a 96-well cell culture plate (2×10^4 cells per well) and were cultured with DMEM plus 10% FBS for 24 h at 37°C, 5% CO_2. Following sterile filtration, drug-loaded nanoparticles were added to yield a series of concentrations from 0.3125 mg/mL to 20 mg/mL, and the cultures were incubated for an additional 24 h. 10 μL of WST-8 solution and 100 μL media were then added to each well. After a 90 min incubation period, absorbance was measured with a Synergy 2 multimode microplate reader (BioTek Instruments, Winooski, VT) at 450 nm. The cytotoxicities of free TMC and TMC-PSA nanoparticles without drug were also evaluated. IC_{50} values were determined using the Hill slope model with Kaleidagraph software. Each experiment was repeated independently at least three times.

Cellular Uptake of Nanoparticles *In Vitro*

Fluorescently-labeled TMC was synthesized by dissolving 15 mg of TMC in 3 ml of 0.1 M sodium bicarbonate buffer (pH 8.3), followed by the addition of 400 μl of Alexa Fluor® 488 carboxylic acid, succinimidyl ester, mixed isomers in DMSO (1 mg/ml). After stirring at room temperature for 1 h with protection from the light, the solution was dialyzed against DI water (Spectrum Laboratories, Inc., MWCO = 6–8 kDa) for 48 h. Removal of unreacted, water soluble Alexa Fluor® 488 was ensured through use of a dialysis membrane with a large molecular weight cut off. Furthermore, due to the excess of reactive amine groups on TMC relative to Alexa Fluor® 488, the amount of unreacted tag was presumed to be negligible. Fluorescently-labeled TMC was isolated by lyophilization, and conjugation of the fluorescent moiety to TMC was verified by ^{1}H NMR (see Supplementary Material Fig. S2);. The isolated, fluorescently labeled TMC was complexed with PSA as described above.

To observe nanoparticle internalization, SW-982 cells were seeded onto lysine-coated 35 mm Glass Bottom Culture Dishes (MatTek Corporation, Ashland, MA) at a density of 1 million cells/dish. The lysine coating was necessary to prevent undesirable adhesion of the positively charged nanoparticles to the plate. After a 24 h incubation period in DMEM plus 10% FBS at 37°C and 5% CO_2, the media was removed, and sterile-filtered, fluorescently-labeled PSA-TMC nanoparticles in 1X PBS were added. Media from the control cells that did not receive nanoparticles was simultaneously replaced with PBS. Cells were incubated for an additional 30 min at 37°C and washed with PBS three times before imaging with a Nikon Eclipse Ti inverted microscope.

In Vitro Assessment of Bioactivity

SW-982 cells were seeded into a 96-well cell culture plate (5,000 cells/well) in the presence of a pro-inflammatory simulant, interleukin-1β (IL-1β) (R&D Systems, Minneapolis, MN), at a concentration of 1 ng/mL. The low concentration of the stimulating agent was able to induce a significant pro-inflammatory response from synovial cells, consistent with previous studies (24–27). After 24 h of incubation, MTX- or DM-loaded nanoparticles were added to the IL-1β stimulated cells following sterile filtration. Prior to addition, the MTX- or DM-loaded nanoparticles were suspended in DMEM plus 10% FBS at a concentration of 1.0 mg/ml. Control groups included stimulated cells without treatment, stimulated cells with addition of free (unloaded) nanoparticles, and stimulated cells with 0.1 mg/mL or 1.0 mg/ml DMARD. After 24 h, culture supernatant was collected and stored in aliquots at −80°C until pro-inflammatory protein analysis. Supernatant samples were analyzed for pro-inflammatory proteins (IL-6, IL-8, and GM-CSF) using a Bio-Plex Precision Pro human cytokine assay panel (BIO-RAD, Hercules, CA) on a Luminex® 200 system (Austin, TX) following a manufacturer-provided protocol. Each experiment was repeated independently at least three times.

Data Analysis

Proteins levels are expressed relative to those obtained from untreated control cells. Data is presented as the mean ± standard deviation (N≥3). All treatment groups (untreated control, 0.1 mg/mL MTX or DM, 1.0 mg/mL MTX or DM, MTX- or DM- loaded nanoparticles, free nanoparticles) were compared by one-way ANOVA with Fisher's LSD post hoc tests. $p<0.05$ was considered to be significant.

RESULTS

Preparation and Characterization of DMARD-Loaded PSA-TMC Nanoparticles

The loading efficiency and loading capacity of PSA-TMC nanoparticles for DM were determined to be 41.3±7% and 0.10±0.02 mg DM/mg nanoparticles, respectively. The values are comparable to those previously obtained in the preparation of MTX-loaded PSA-TMC nanoparticles (LE= 46.3±13%, LC=0.10±0.03 mg MTX/mg nanoparticles) (13).

Likewise, as provided in Table I, the size of DM-loaded nanoparticles was slightly greater than that previously observed for free nanoparticles and comparable to that determined for MTX-loaded nanoparticles. All of the nanoparticle formulations yielded a low polydispersityand a zeta potential value greater than 30 mV. The slight increase in size, in conjunction with the lack of an observable effect on zeta potential, indicates that the DMARDs were being entrapped within the nanosized carriers, as expected.

Table I Physical Characterization of DMARD-Loaded Nanoparticles

	Size (nm)	Zeta potential (mV)	PDI
PSA-TMC Nanoparticles	102.2±14.5	33.4±1.6	0.12±0.02
MTX-loaded Nanoparticles	128.7±5.3	32.7±0.9	0.10±0.02
DM-loaded Nanoparticles	120.7±11.1	34.8±2.5	0.12±0.02

Fractional release of DM from the PSA-TMC nanoparticles (Fig. 1) mirrored that previously observed for MTX (13). The release profile was fit to the following equation derived from Fick's second law assuming a spherical geometry, a homogeneous distribution of drug within the nanoparticle, and a constant nanoparticle radius:

$$\frac{m_{DM}(t)}{m_{DM,0}} = \frac{6}{\pi^2}\sum_{n=1}^{\infty}\frac{1}{n^2}e^{\frac{-D_{DM}n^2\pi^2 t}{R^2}} \quad (3)$$

where D_{DM} is the diffusion coefficient, R is the nanoparticle radius, t is the time in seconds, and $m_{DM}(t)$ and $m_{DM,0}$ are the masses of DM at times t and $t=0$, respectively, that remain in the nanoparticle. As indicated by the inset of Fig. 1, the diffusion model did not describe the experimental data well during the initial period of release . The latter deficiency in the model, in conjunction with a low calculated diffusion coefficient of 9.02×10^{-13} cm^2/s, suggests that drug dissolution prior to diffusion is the rate limiting factor in controlled release from the nanoparticle (28).

In Vitro Cytotoxicity PSA-TMC Nanoparticles

As summarized Table II with the calculated IC_{50} values, the free and DMARD-loaded nanoparticles were non-cytotoxic towards the SW-982 cells up to high concentrations. Consistent with our prior study using MH7A synovial cells, the inherent cytotoxicity of quaternized chitosan was significantly reduced upon complexation with PSA to form nanoparticles (13). Free MTX and DM did not have a significant impact on cellular proliferation up to the maximum concentration tested (4 mg/ml) (see Supplementary Material Fig. S1); therefore, IC_{50} values for the free drugs could not be calculated. Of note, the IC_{50} value for the PSA-TMC nanoparticles did not change with DMARD loading, providing additional evidence that MTX and DM do not impact cellular proliferation at the therapeutic concentrations tested. Based upon the established loading capacity of 0.1 mg drug/mg nanoparticles, the free

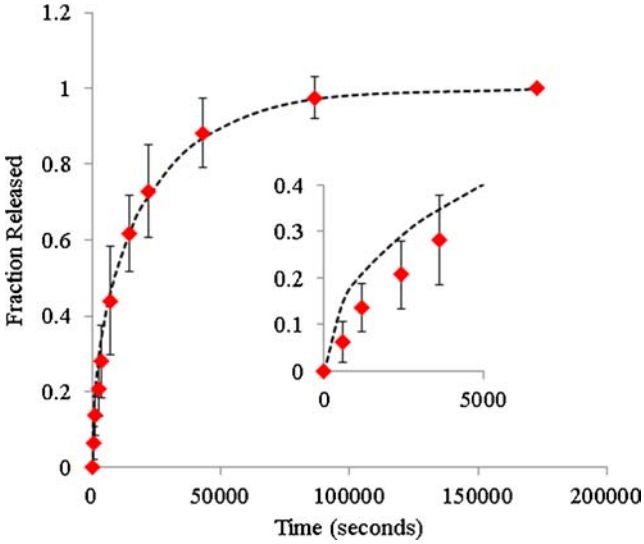

Fig. 1 Fractional release of dexamethasone from PSA-TMC nanoparticles as a function of time. The *dashed line* represents the release profile derived from the diffusion model.

drug concentration was only ~1.5 mg/ml at the IC_{50} values determined for the drug-loaded nanoparticles.

Cellular Uptake of Nanoparticles *In Vitro*

By modifying TMC with a green fluorescent tag prior to nanoparticle formation, uptake of the PSA-TMC cells by synovial SW-982 cells could be observed with the aid of a fluorescent, inverted microsope. As illustrated in Fig. 2, the nanoparticles acculmulated within the cells following a short incubation period (~30 min).

In Vitro Assessment of Bioactivity

MTX-loaded nanoparticles significantly suppressed IL-8 secretion relative to the untreated control group (Fig. 3). The amount of IL-8 suppression was comparable to that achieved with low concentration (0.1 mg MTX/ml) and high concentration (1.0 mg MTX/ml) MTX treatment. Low and high concentration MTX treatment also showed significant inhibition of GM-CSF secretion as compared to the untreated control group, the MTX-loaded nanoparticle group, and the free nanoparticle group. Free MTX treatment (low and high concentration) also resulted in a significant decrease in IL-6 secretion relative to the free nanoparticle group; however, a significant difference from the untreated control group was not observed, and only high concentration MTX treatment yielded a significant reduction from the MTX-loaded nanoparticle group. The nanoparticles alone significantly increased GM-CSF secretion, although this effect was diminished through incorporation of MTX.

DM-loaded nanoparticles significantly suppressed IL-6 and IL-8 secretion relative to the untreated control group and had comparable efficacy to low (0.1 mg DM/ml) and high (1.0 mg DM/ml) concentration free DM treatment (Fig. 4). For IL-6, a significant difference was also observed for groups that received free DM treatment or DM-loaded nanoparticle treatment relative to the free nanoparticle group. Furthermore, although there was no significant difference from the control, treatment with DM-loaded nanoparticles, low concentration free DM, and high concentration free DM resulted in significantly lower GMC-SF levels relative to treatment with free nanoparticles.

Table II IC_{50} Values for TMC, PSA-TMC Nanoparticles, and DMARD-Loaded Nanoparticles

	IC_{50} (mg/ml)
TMC	5.16 ± 0.20
PSA-TMC Nanoparticles	15.82 ± 1.44
MTX	−−*
DM	−−*
MTX-loaded Nanoparticles	14.20 ± 1.20
DM-loaded Nanoparticles	16.01 ± 0.42

*MTX and DM did not significantly impact cellular proliferation over the range of concentrations tested

DISCUSSION

Drug carrier systems offer a solution to the drawbacks, such as low solubility, unpredictable pharmacokinetics, and non-site specific distribution, commonly associated with conventional DMARDs that often result in adverse side effects (4–6). In the current study, an *in vitro* model of RA based upon IL-1β activated synovial fibroblasts, the so-called conductors of joint destruction (29,30), was used to demonstrate that the bioactivity of DMARDs can be maintained when loaded into PSA-TMC nanoparticles.

In accord with our prior study (13), DMARD-loaded nanoparticles were successfully prepared *via* combination of TMC with PSA in the presence of TPP and MTX or DM. Electrostatic interaction of the positively charged ammonium groups of TMC with the negatively charged carboxylic acid groups of PSA results in charge neutralization, a consequent reduction in hydrophilicity, and the formation of stable, intermolecular complexes (31–33). While an in-depth analysis of mechanism is beyond the scope of the current study, the high flexibility of PSA in solution is thought to result in an enhanced ability to conformationally match with TMC that, in turn, allows for the formation of a smaller particle size relative to nanoparticles formed from the combination of chitosan or TMC with other anionic polysaccharides (31). The inclusion of TPP, although not required for nanoparticle formation, facilitates inter- and intra-molecular crosslinking of the chitosan, which consequently results in a narrower size distribution and

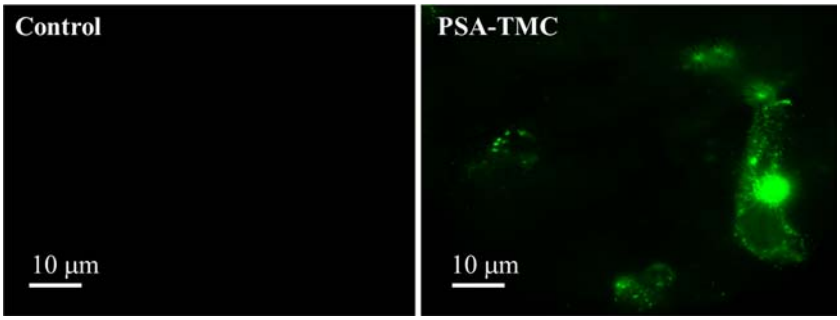

Fig. 2 Color composite of fluorescence microscopy images demonstrating nanoparticle uptake at room temperature by human synovial sarcoma SW-982 cells. To facilitate fluorescence microscopic evaluation, TMC was conjugated to Alexa Fluor® 488 prior to PSA-TMC nanoparticle formation. Use of identical imaging settings permits direct comparison of fluorescence intensities. Higher intensities indicated more cellular uptake of nanoparticle by cells. *Left image*: cells not incubated with nanoparticles results in negligible signal. *Right image*: cells incubated with nanoparticles and showed active cellular uptake. Both groups were incubated for 30 min and washed three times with PBS before imaging.

enhanced stability (32,33). As discussed in greater depth elsewhere, the observed sizes and zeta potentials obtained for DMARD-loaded nanoparticles (Table I) are expected to minimize accumulation within healthy tissue, reduce undesirable uptake by the reticuloendothelial system, and facilitate delivery to the inflamed tissue by exploiting the leaky vasculature that characterizes RA (13).

Similar to what was previously observed for fractional release of MTX from the nanoparticles, controlled release of DM was facilitated over a 24 h period (13). As indicated by the inset of Fig. 1, the diffusion model (Eq. 3) did not describe the experimental data well during the initial period of release. The latter deficiency in the model, in conjunction with a low calculated diffusion coefficient of 9.02×10^{-13} cm^2/s, suggests that drug dissolution prior to diffusion is the rate limiting factor in controlled release from the nanoparticle (28). A slow release rate is desirable in order to provide the nanoparticles with sufficient time to accumulate within the targeted tissue without a significant loss of entrapped drug.

While some toxicity is permissible in carrier systems designed for cancer therapy, the primary goal of inflammation reduction in RA treatment demands minimal toxicity. Consistent with our previous studies using the MH7A synovial fibroblast cell line (13), the free DMARDs, the PSA-TMC nanoparticles, and the DMARD-loaded PSA-TMC nanoparticles showed negligible cytotoxicity towards the synovial SW-982 cell line up to high concentrations. The SW-982 cell line was used in lieu of the MH7A cell line in the current study due to evidence suggesting that the MH7A cell line may not accurately mimic the cytokine profile observed RA (27).

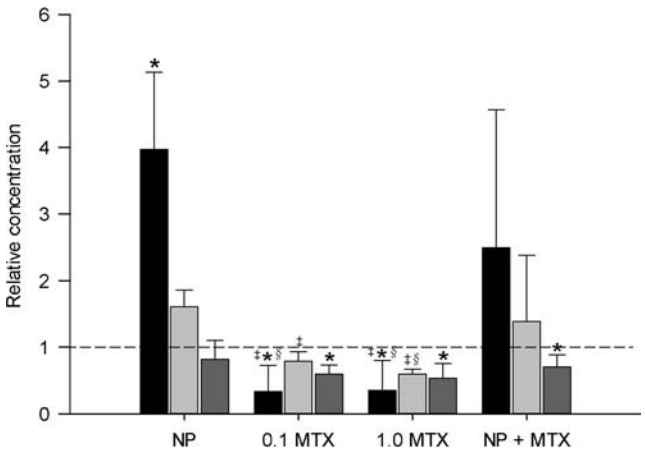

Fig. 3 Relative protein secretion (*black*: GM-CSF; *grey*: IL-6; *dark grey*: IL-8) of IL-1β-stimulated SW-982 cells after treatment with free nanoparticles (NP) at a concentration of 1.0 mg/ml, free MTX at a concentration of 0.1 mg/ml (0.1 MTX), free MTX at a concentration of 1.0 mg/ml (1.0 MTX), and MTX-loaded nanoparticles at a concentration of 1.0 mg/ml (NP + MTX). The *dashed line* at a relative concentration of 1 is intended to serve as a point of reference for unstimulated control cells. * indicates a significant difference *versus* untreated control cells ($p < 0.05$); ‡ indicates a significant difference *versus* free nanoparticles ($p < 0.05$); and § indicates a significant difference *versus* MTX-loaded nanoparticles ($p < 0.05$).

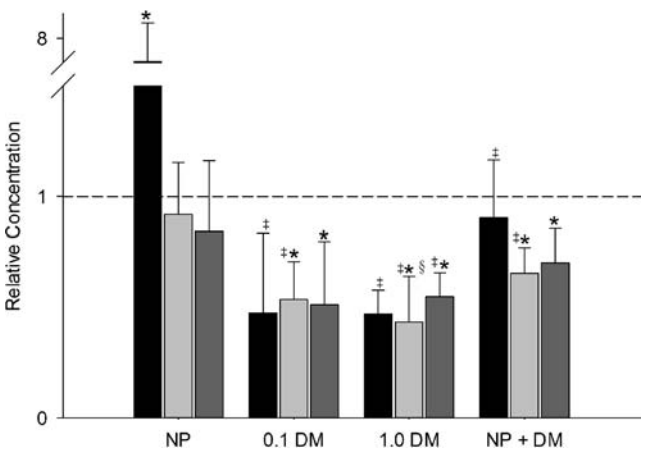

Fig. 4 Relative protein secretion (*black*: GM-CSF; *grey*: IL-6; *dark grey*: IL-8) of IL-1β-stimulated SW-982 cells after treatment with free nanoparticles (NP) at a concentration of 1.0 mg/ml, free DM at a concentration of 0.1 mg/ml (0.1 DM), free DM at a concentration of 1.0 mg/ml (1.0 DM), and DM-loaded nanoparticles at a concentration of 1.0 mg/ml (NP + DM). The *dashed line* at a relative concentration of 1 is intended to serve as a point of reference for unstimulated control cells. * indicates a significant difference *versus* untreated control cells ($p < 0.05$); ‡ indicates a significant difference *versus* free nanoparticles ($p < 0.05$); and § indicates a significant difference *versus* DM-loaded nanoparticles ($p < 0.05$).

Furthermore, the SW-982 cell line was shown to accurately mimic expression of the proinflammatory mediator associated with RA, including IL-6 and IL-8, particularly after stimulation with IL-1β (24–26). The negligible impact of MTX and DM on the IC_{50} values suggests that any changes in the secretion of proinflammatory mediators observed for the *in vitro* model of RA were due to cellular response rather than apoptosis. As illustrated in Fig. 2, the PSA-TMC nanoparticles were internalized by SW-982 cells. This result confirmed the potential for intracellular delivery of therapeutics *via* PSA-TMC nanoparticles even in the absence of a targeting moiety that would facilitate receptor-mediated endocytotic uptake.

Changes in the secretion of IL-6, IL-8, and GM-CSF by the activated SW-982 cells were used to demonstrate that DMARDs loaded into nanoparticles retained bioactivity and were able to reduce the inflammatory response (Figs. 3,4). IL-6, IL-8, and GM-CSF were selected as representative cytokines, chemokines, and growth factors, respectively. A literature survey suggested that the three chosen proteins are critical to the pathogenesis of RA (23). IL-6 is involved in in immune regulation, inflammation, and hematopoiesis. More specifically, IL-6 is thought to simulate T and B cells (23,34), activate osteoclasts, and induce expression of vascular endothelial growth factor (VEGF) (34), which subsequently triggers the angiogenesis that, in part, characterizes RA. IL-8 stimulates the migration of inflammatory cells into the synovium, actives synovial fibroblasts *via* an autocrine mechanism to induce secretion of additional pro-inflammatory mediators, and promotes angiogenesis (35,36). GM-CSF recruits and activates inflammatory cells, particularly T-cells, while also inhibiting differentiation of osteoclasts (23) . When administered *in vivo*, DMARDs, including those used in the current study, have been shown to reduce the levels of the select pro-inflammatory mediators, thereby disrupting the pro-inflammatory network associated with RA (37–39).

Despite the observations made *in vivo*, *in vitro* administration of MTX has yielded variable responses. Although MTX is as a folate antagonist in the treatment of cancer, the mechanism of action for MTX in the treatment of RA is unclear (40–42) and the inconsistencies in *in vitro* response reflect this lack of understanding. For example, while Sung *et al.* reported a significant reduction in IL-6 expression and secretion by activated synovial cells upon treatment with low-concentration MTX (43), Inoue *et al.* and Seitz *et al.* reported that MTX had no or marginal impact on IL-6 or IL-8 production (44,45). The conflicting results suggest that alterations in the cytokine milieu observed *in vivo* may not be a direct result of MTX administration (46).

In contrast to MTX, *in vitro* administration of DM has yielded consistent, reproducible results that correlate with *in vivo* observations. DM is believed to reduce inflammation in the same manner as other glucocorticoids, where by binding to a glucocorticoid receptor (GR) directly impacts the activity of activator protein-1 (AP-1) and nuclear factor kappaB (NF-κB) (47). The latter transcription factors have been definitively linked to the expression and secretion of most pro-inflammatory cytokines and chemokines, including IL-6, IL-8, and GM-CSF (48–50). In agreement with the latter posited mechanism, several investigators have noted that *in vitro* expression of IL-6 and IL-8 by activated synovial cells is significantly reduced following exposure to DM (37,45,51). Likewise, GM-CSF secretion has also been reduced, although not to the same degree as IL-6 and IL-8 (52,53). In light of the observations made by other investigators concerning the variable *in vitro* anti-inflammatory activity of MTX and the established strong anti-inflammatory activity of DM, we chose to observe the impact of both therapeutics loaded into PSA-TMC nanoparticles in the current study.

Based upon the results and the cytotoxicity studies, a concentration of 1 mg/ml was used for *in vitro* studies to ensure an observable response without impacting cellular viability. Furthermore, although the two concentrations of DMARD used in this study are designated as low and high, the concentrations of MTX used were similar to those used by other investigators studying the *in vitro* impact of low concentration MTX on RA (43). When applied to our *in vitro* model of RA, the DM- and MTX-loaded nanoparticles, as well as the free DMARDs, yielded significant reductions in the secretion of IL-8 relative to the control, while only DM (free or encapsulated within nanoparticle) led to significantly decreased IL-6 levels relative to the control. In contrast, MTX (free and encapsulated) did not affect IL-6 concentrations relative to the control group, although significant differences were observed comparing treatment with free nanoparticles to free DMARDs. The latter results are reflective of the potential differences in the mechanism of action of MTX and DM, as noted above, and are in agreement with the observations of Inoue *et al.* and Seitz *et al.* (44,45).

For GM-CSF, only free MTX yielded an observable decrease in GM-CSF levels, although free DM showed a non-significant reduction. Surprisingly, free nanoparticles significantly enhanced GM-CSF secretion, although this effect was somewhat diminished by incorporation of the DMARDs, particularly DM. Carriers based upon chitosan and chitosan derivatives are often reported as being non-immunogenic (54); however, a careful search of the literature revealed that in some cell types chitosan-based nanoparticles can induce or enhance an inflammatory response (55–57). For example, administration of chitosan nanoparticles to bone-derived macrophages led to increased and variable secretion of GM-CSF, with little impact on IL-6 secretion (55). Given the positive results obtained for IL-6 and IL-8, this possible induction of a response by the SW-982 cells does not diminish the potential of the PSA-TMC nanoparticles; however, a more thorough evaluation of changes in the cytokine profile resultant from the particles alone may be necessary prior to *in vivo* experiments.

Of note, there were no significant differences in the concentrations of IL-6 and IL-8 when comparing the free DMARDs and DMARD-loaded nanoparticles, administered at concentration of 0.1 mg/ml and 1.0 mg/ml, respectively. Based on the loading capacity of the DMARD nanoparticles (0.1 mg/mg), the free DMARDs were administrated at equal weight concentration relative to the DMARDs within the nanoparticles. Thus, the results suggest that DMARDs loaded into nanoparticles are able to retain bioactivity. Ideally, the nanoparticles would have enhanced the therapeutic efficacy of entrapped DMARDs; however, when applied *in vivo* the ability of the nanoparticles to passively target the diseased tissue is anticipated to lead towards greater and more predictable anti-inflammatory responses of the entrapped therapeutics.

CONCLUSION

PSA-TMC nanoparticles were previously developed for targeted delivery in the treatment of RA to reduce the non-specific cytotoxicity of DMARDs. The physical characteristics and DMARD-loading capacity of the nanoparticles were suggestive of a suitable carrier system. In this study, an RA *in vitro* model was used to validate that two common DMARDs, MTX and DM, retain bioactivity and are able to elicit a an anti-inflammatory therapeutic response when entrapped in nanoparticles. The present study provides the foundation for future studies aimed towards (1) improving the site-specificity of the nanoparticles through surface modification with a targeting ligand and (2) demonstrating *in vivo* that the nanoparticles can be used to enhance the efficacy of entrapped DMARDs through targeted delivery.

ACKNOWLEDGMENTS AND DISCLOSURES

We thank David Wilson for assistance with the HPLC in evaluating controlled release of DM from the nanoparticles. Cellular uptake of the nanoparticles was observed under the direction of Dr. Martin B. Forstner. This work was supported by NSF grant CBET-1032506.

REFERENCES

1. Lindholm A, Kahan BD. Influence of cyclosporine pharmacokinetics, trough concentrations, and AUC monitoring on outcome after kidney transplantation. Clin Pharmacol Ther. 1993;54(2):205–18.
2. Weinblatt ME, Kremer JM. Methotrexate in rheumatoid arthritis. J Am Acad Dermatol. 1988;19(1 Pt 1):126–8.
3. Mottram PL. Past, present and future drug treatment for rheumatoid arthritis and systemic lupus erythematosus. Immunol Cell Biol. 2003;81(5):350–3.
4. Goodman TA, Polisson RP. Methotrexate: adverse reactions and major toxicities. Rheum Dis Clin N Am. 1994;20(2):513–28.
5. Wolverton SE, Remlinger K. Suggested guidelines for patient monitoring: hepatic and hematologic toxicity attributable to systemic dermatologic drugs. Dermatol Clin. 2007;25(2):195–205. vi–ii.
6. Baschant U, Lane NE, Tuckermann J. The multiple facets of glucocorticoid action in rheumatoid arthritis. Nat Rev Rheumatol. 2012;8(11):645–55.
7. Liu Z, Jiao Y, Wang Y, Zhou C, Zhang Z. Polysaccharides-based nanoparticles as drug delivery systems. Adv Drug Deliv Rev. 2008;60(15):1650–62.
8. Prabaharan M, Mano JF. Chitosan-based particles as controlled drug delivery systems. Drug Deliv. 2005;12(1):41–57.
9. Ko JA, Park HJ, Hwang SJ, Park JB, Lee JS. Preparation and characterization of chitosan microparticles intended for controlled drug delivery. Int J Pharm. 2002;249(1–2):165–74.
10. Janes KA, Fresneau MP, Marazuela A, Fabra A, Alonso MJ. Chitosan nanoparticles as delivery systems for doxorubicin. J Control Release. 2001;73(2–3):255–67.
11. Fernandez-Urrusuno R, Calvo P, Remunan-Lopez C, Vila-Jato JL, Alonso MJ. Enhancement of nasal absorption of insulin using chitosan nanoparticles. Pharm Res. 1999;16(10):1576–81.
12. Katas H, Alpar HO. Development and characterisation of chitosan nanoparticles for siRNA delivery. J Control Release. 2006;115(2):216–25.
13. Zhang N, Bader RA. Synthesis and characterization of polysialic acid-N-Trimethyl chitosan nanoparticles for drug delivery. NanoLIFE. 2012;2(3):1241003.
14. Jain S, Hreczuk-Hirst DH, McCormack B, Mital M, Epenetos A, Laing P, *et al.* Polysialylated insulin: synthesis, characterization and biological activity in vivo. Biochim Biophys Acta. 2003;1622(1):42–9.
15. Fernandes AI, Gregoriadis G. The effect of polysialylation on the immunogenicity and antigenicity of asparaginase: implication in its pharmacokinetics. Int J Pharm. 2001;217(1–2):215–24.
16. Fernandes AI, Gregoriadis G. Polysialylated asparaginase: preparation, activity and pharmacokinetics. Biochim Biophys Acta. 1997;1341(1):26–34.
17. Fernandes AGG. FC41 catalase-polysialic acid conjugates. Eur J Pharm Sci. 1994;2(1–2):111.
18. Fernandes AI, Gregoriadis G. Synthesis, characterization and properties of sialylated catalase. Biochim Biophys Acta. 1996;1293(1):90–6.
19. Gregoriadis G, Jain S, Papaioannou I, Laing P. Improving the therapeutic efficacy of peptides and proteins: a role for polysialic acids. Int J Pharm [Article]. 2005;300(1-2):125–30.
20. Gregoriadis G, Fernandes A, Mital M, McCormack B. Polysialic acids: potential in improving the stability and pharmacokinetics of proteins and other therapeutics. Cell Mol Life Sci. 2000;57(13–14):1964–9.
21. Gregoriadis G, Fernandes A, McCormack B, Mital M, Zhang X. Polysialic acids: potential role in therapeutic constructs. Biotechnol Genet Eng Rev. 1999;16:203–15.
22. Ritchlin C. Fibroblast biology. Effector signals released by the synovial fibroblast in arthritis. Arthritis Res. 2000;2(5):356–60.
23. McInnes IB, Schett G. Cytokines in the pathogenesis of rheumatoid arthritis. Nat Rev Immunol. 2007;7(6):429–42.
24. Yamazaki T, Yokoyama T, Akatsu H, Tukiyama T, Tokiwa T. Phenotypic characterization of a human synovial sarcoma cell line, SW982, and its response to dexamethasone. In Vitro Cell Dev Biol-Anim. 2003;39(8-9):337–9.
25. Choi EM, Lee YS. Luteolin suppresses IL-1 beta-induced cytokines and MMPs production via p38 MAPK, JNK, NF-kappaB and AP-1 activation in human synovial sarcoma cell line, SW982. Food Chem Toxicol. 2010;48(10):2607–11.
26. Wada Y, Shimada K, Kimura T, Ushiyama S. Novel p38 MAP kinase inhibitor R-130823 suppresses IL-6, IL-8 and MMP-13 production in spheroid culture of human synovial sarcoma cell line SW 982. Immunol Lett. 2005;101(1):50–9.

27. Wagoner KL, Bader RA. Evaluation of SV40-transformed synovial fibroblasts in the study of rheumatoid arthritis pathogenesis. Rheumatol Int. 2012;32(7):1885–91.
28. Polakovic M, Gorner T, Gref R, Dellacherie E. Lidocaine loaded biodegradable nanospheres. II. Modelling of drug release. J Control Release. 1999;60(2–3):169–77.
29. Huber LC, Distler O, Tarner I, Gay RE, Gay S, Pap T. Synovial fibroblasts: key players in rheumatoid arthritis. Rheumatology (Oxford). 2006;45(6):669–75.
30. Pap T, Muller-Ladner U, Gay RE, Gay S. Fibroblast biology. Role of synovial fibroblasts in the pathogenesis of rheumatoid arthritis. Arthritis Res. 2000;2(5):361–7.
31. Boddohi S, Moore N, Johnson PA, Kipper MJ. Polysaccharide-based polyelectrolyte complex nanoparticles from chitosan, heparin, and hyaluronan. Biomacromolecules. 2009;10(6):1402–9.
32. Janes KA, Calvo P, Alonso MJ. Polysaccharide colloidal particles as delivery systems for macromolecules. Adv Drug Deliv Rev. 2001;47(1):83–97.
33. Nagpal K, Singh SK, Mishra DN. Chitosan nanoparticles: a promising system in novel drug delivery. Chem Pharm Bull (Tokyo). 2010;58(11):1423–30.
34. Nakahara H, Song J, Sugimoto M, Hagihara K, Kishimoto T, Yoshizaki K, *et al.* Anti-interleukin-6 receptor antibody therapy reduces vascular endothelial growth factor production in rheumatoid arthritis. Arthritis Rheum. 2003;48(6):1521–9.
35. Nanki T, Nagasaka K, Hayashida K, Saita Y, Miyasaka N. Chemokines regulate IL-6 and IL-8 production by fibroblast-like synoviocytes from patients with rheumatoid arthritis. J Immunol. 2001;167(9):5381–5.
36. Koch AE. Chemokines and their receptors in rheumatoid arthritis future targets? Arthritis Rheum. 2005;52(3):710–21.
37. Seitz M, Loetscher P, Dewald B, Towbin H, Rordorf C, Gallati H, *et al.* Methotrexate action in rheumatoid arthritis: stimulation of cytokine inhibitor and inhibition of chemokine production by peripheral blood mononuclear cells. Br J Rheumatol. 1995;34(7):602–9.
38. Maillefert JF, Puechal X, Falgarone G, Lizard G, Ornetti P, Solau E, *et al.* Prediction of response to disease modifying antirheumatic drugs in rheumatoid arthritis. Joint Bone Spine. 2010;77(6):558–63.
39. Cutolo M, Sulli A, Pizzorni C, Seriolo B, Straub RH. Anti-inflammatory mechanisms of methotrexate in rheumatoid arthritis. Ann Rheum Dis. 2001;60(8):729–35.
40. Chan ESL, Cronstein BN. Methotrexate-how does it really work? Nat Rev Rheumatol. 2010;6(3):175–8.
41. Chan ESL, Cronstein BN. Molecular action of methotrexate in inflammatory diseases. Arthritis Res. 2002;4(4):266–73.
42. Cronstein BN. Low-dose methotrexate: a mainstay in the treatment of rheumatoid arthritis. Pharmacol Rev. 2005;57(2):163–72.
43. Sung JY, Hong JH, Kang HS, Choi I, Lim SD, Lee JK, *et al.* Methotrexate suppresses the interleukin-6 induced generation of reactive oxygen species in the synoviocytes of rheumatoid arthritis. Immunopharmacology. 2000;47(1):35–44.
44. Seitz M, Loetscher P, Dewald B, Towbin H, Baggiolini M. In vitro modulation of cytokine, cytokine inhibitor, and prostaglandin E release from blood mononuclear cells and synovial fibroblasts by antirheumatic drugs. J Rheumatol. 1997;24(8):1471–6.
45. Inoue H, Takamori M, Nagata N, Nishikawa T, Oda H, Yamamoto S, *et al.* An investigation of cell proliferation and soluble mediators induced by interleukin 1beta in human synovial fibroblasts: comparative response in osteoarthritis and rheumatoid arthritis. Inflamm Res. 2001;50(2):65–72.
46. Swierkot J, Szechinski J. Methotrexate in rheumatoid arthritis. Pharmacol Rep. 2006;58(4):473–92.
47. Scheinman RI, Gualberto A, Jewell CM, Cidlowski JA, Baldwin AS. Characterization of mechanisms involved in transrepression of NF-Kappa-B by activated glucocorticoid receptors. Mol Cell Biol. 1995;15(2):943–53.
48. Barnes PJ, Adcock IM. How do corticosteroids work in asthma? Ann Intern Med. 2003;139(5):359–70.
49. Leung DYM, Bloom JW. Update on glucocorticoid action and resistance. J Allergy Clin Immunol. 2003;111(1):3–23.
50. Muller-Ladner U, Nishioka K. p53 in rheumatoid arthritis: friend or foe? Arthritis Res. 2000;2(3):175–8.
51. Tan PL, Farmiloe S, Yeoman S, Watson JD. Expression of the interleukin 6 gene in rheumatoid synovial fibroblasts. J Rheumatol. 1990;17(12):1608–12.
52. Filonzi EL, Zoellner H, Stanton H, Hamilton JA. Cytokine regulation of granulocyte-macrophage colony stimulating factor and macrophage colony-stimulating factor production in human arterial smooth muscle cells. Atherosclerosis. 1993;99(2):241–52.
53. Hamilton JA, Piccoli DS, Cebon J, Layton JE, Rathanaswani P, McColl SR, *et al.* Cytokine regulation of colony-stimulating factor (CSF) production in cultured human synovial fibroblasts. II. Similarities and differences in the control of interleukin-1 induction of granulocyte-macrophage CSF and granulocyte-CSF production. Blood. 1992;79(6):1413–9.
54. Rodrigues S, Dionisio M, Lopez CR, Grenha A. Biocompatibility of chitosan carriers with application in drug delivery. Funct Biomater. 2012;3:615–41.
55. Guzman-Morales J, Ariganello MB, Hammami I, Thibault M, Jolicoeur M, Hoemann CD. Biodegradable chitosan particles induce chemokine release and negligible arginase-1 activity compared to IL-4 in murine bone marrow-derived macrophages. Biochem Biophys Res Commun. 2011;405(4):538–44.
56. Witschi C, Mrsny RJ. In vitro evaluation of microparticles and polymer gels for use as nasal platforms for protein delivery. Pharm Res. 1999;16(3):382–90.
57. Li X, Min M, Du N, Gu Y, Hode T, Naylor M, *et al.* Chitin, chitosan, and glycated chitosan regulate immune responses: the novel adjuvants for cancer vaccine. Clin Dev Immunol. 2013;2013:387023.